APPLICATION OF TAGUCHI METHOD IN THE OPTIMIZATION OF LASER MICRO-ENGRAVING OF PHOTOMASKS

Y. H. Chen[1], S. C. Tam[2], W. L. Chen[1] and H. Y. Zheng[1]
(1) Gintic Institute of Manufacturing Technology
Nanyang Technological University
71 Nanyang Drive, Singapore 638075 Fax: (65)792-2779
(2) School of Electrical & Electronic Engineering
Nanyang Technological University
Nanyang Avenue, Singapore 639798

Abstract: Photomasks are needed to generate various design patterns in the fabrication of liquid crystal displays (LCDs). This paper discusses the use of the Taguchi method of experimental design in optimising process parameters for micro-engraving of iron oxide coated glass using a Q-switched Nd:YAG laser. The effects of five key process parameters - beam expansion ratio, focal length, average laser power, pulse repetition rate and engraving speed - have been explored. The primary response under study is the engraving linewidth. An L16 orthogonal array was used to accommodate the experiments. The study indicated that a minimum linewidth of 18 μm could be obtained with beam expansion ratio of 5 ×, focal length of 50mm, laser average power of 0.4 W, pulse repetition rate of 5 kHz, and engraving speed of 5000 mm/min.

Keywords: Laser engraving, photomasks, Taguchi method, parameter optimisation

1 INTRODUCTION

Integrated circuit fabrication requires a long sequence of many complex processes. Lithography is one of these complex processes as it is used to define dimensions, doping, and interconnection of devices. The types of lithography may be primarily categorised according to exposure radiation as optical, X-ray, e-beam and ion beam. Each lithography system requires a substantial amount of supporting equipment, including masks and mask making equipment [1,2]. Photoreduction is a standard technique for mask making, but it is labour intensive and expensive because of the many steps involved. Lasers have been used in fabricating masks, either as a light source for photolithography or as a direct writing tool [3,4]. For mask making with a linewidth wider than 4μm, the latter is more effective and economical as direct-writing is a one-step process [5].

The photomask is usually made of a glass substrate coated with a film. In this project, engraving to remove the film at the selected areas is performed with a Nd:YAG laser beam operating at 1.06μm. The metal removal is the result of thermal heating of the coated film. The process includes several interactions, including absorption of laser radiation by the film, absorption and reflection of laser radiation by the substrate, heat transfer from film to substrate, plasma coupling and explosive effect [6,7]. The process performance is affected by laser system parameters, such as laser peak power, average power, pulse repetition rate, beam expansion ratio, focal length of the focusing lens, depth of the beam focus with respect to the surface of the photomask, and engraving speed. Optimisation of these factors will produce the best possible engraving quality without an increase of cost. Taguchi method is a robust technique that can be used to analyse the significance of each control factor, to evaluate the process performance, and to optimise parameters to obtain a minimum linewidth [8].

2 TAGUCHI METHOD

There are many ways to design a test, but the most frequently used approach is a full factorial experiment. However, for full factorial experiments, there are 2^f possible combinations that must be tested (f=the

number of factors each at two levels). Therefore, it is very time-consuming when there are many factors [8].

In order to minimise the number of tests required, fractional factorial experiments (FFEs) were developed. FFEs use only a portion of the total possible combinations to estimate the effects of main factors and the effects of some of the interactions. Taguchi developed a family of FFE matrices which could be utilised in various situations. These matrices reduce the experimental number but still obtain reasonably rich information. The conclusions can also be associated with statistical level of confidence.

In Taguchi's methodology, all factors affecting the process quality can be divided into two types: control factors and noise factors [8,9,10]. Control factors are those set by the manufacturer and are easily adjustable. These factors are most important in determining the quality of product characteristics. Parametric optimisation in laser micro-engraving is to find out the main control factors and select their appropriate levels. For the hardware used in this project, typical control factors include average laser power, engraving speed, pulse repetition rate, beam expansion ratio and lens focal length. Noise factors , on the other hand, are those undesired variables that are difficult, impossible, or expensive to control, such as the ambient temperature, humidity and ageing of parts.

The major steps of implementing the Taguchi method are: (1) to identify the factors/interactions, (2) to identify the levels of each factor, (3) to select an appropriate orthogonal array (OA), (4) to assign the factors/interactions to columns of the OA, (5) to conduct the experiments, (6) to analyse the data and determine the optimal levels, and (7) to conduct the confirmation experiment.

Two-level factors are recommended by Taguchi for an initial experiment. If the factors and interactions are less than 15, a possible matrix is a sixteen-trial orthogonal array, which is labelled an L16 matrix. An L16, two-level matrix is shown in Table 1, where the numbers 1 and 2 stand for the levels of the factors.

In data analysis, signal-to-noise (S/N) ratios are used to allow the control of the response as well as to reduce the variability about the response. The use of ANOVA (analysis of variance) is to calculate the statistical confidence associated with the conclusions drawn.

Table 1 L16 orthogonal array

Trial	Column														
No.	1	2	3	4	5	6	7	8	9	10	11	12	13	14	15
1	1	1	1	1	1	1	1	1	1	1	1	1	1	1	1
2	1	1	1	1	1	1	1	2	2	2	2	2	2	2	2
3	1	1	1	2	2	2	2	1	1	1	1	2	2	2	2
4	1	1	1	2	2	2	2	2	2	2	2	1	1	1	1
5	1	2	2	1	1	2	2	1	1	2	2	1	1	2	2
6	1	2	2	1	1	2	2	2	2	1	1	2	2	1	1
7	1	2	2	2	2	1	1	1	1	2	2	2	2	1	1
8	1	2	2	2	2	1	1	2	2	1	1	1	1	2	2
9	2	1	2	1	2	1	2	1	2	1	2	1	2	1	2
10	2	1	2	1	2	1	2	2	1	2	1	2	1	2	1
11	2	1	2	2	1	2	1	1	2	1	2	2	1	2	1
12	2	1	2	2	1	2	1	2	1	2	1	1	2	1	2
13	2	2	1	1	2	2	1	1	2	2	1	1	2	2	1
14	2	2	1	1	2	2	1	2	1	1	2	2	1	1	2
15	2	2	1	2	1	1	2	1	2	2	1	2	1	1	2
16	2	2	1	2	1	1	2	2	1	1	2	1	2	2	1

3 EXPERIMENT

3.1 Description of Experimental Set-up

Experiments were performed with an NEC M690B Q-switched Nd:YAG laser system. The Nd:YAG laser can produce a maximum average power of 7 W at TEM_{00} mode with an acousto-optic Q-switch element, whose pulse repetition rate can be adjusted from 1 kHz to 50 kHz in steps of 1 kHz. The beam diameter from the laser generator is about 1.8 mm. An attenuator is used to continuously reduce the power from the maximum to 2% of the laser output power. A beam expander is used to enlarge the beam and reduce the far-field divergence angle to get as small a spot size as possible at the focal plane. The X-Y table is driven by CNC drive motors. The photomask is a glass substrate with iron oxide coating. The thickness of the deposited film is about 80 nm, and the thickness of the glass substrate is 1.5 mm.

3.2 Factors and Goals

In laser engraving of photomasks, the desirable results are narrow linewidth, little spattering, small heat-affected-zone, no broken line and high contrast. The present objective of our experiments focuses on narrow linewidth. The cause-and-effect diagram is employed [11] to select the factors. The initial experiments showed that the engraving linewidths marked at the focal position were always narrower than those marked at out of the focus position. Therefore, beam defocus is not included in the list of factors studied in the Taguchi experiment.

Eventually, the following factors are chosen in the experiment: average laser power delivered to the photomask surface, beam expansion ratio, focal length of the processing lens, pulse repetition rate and engraving speed. These factors are the key parameters controlling the focal spot size, overlap ratio, and interaction time. The factors and levels are shown in Table 2.

Table 2 Factors and levels

Symbols and Factors	Level 1	Level 2
A Beam Expansion Ratio (Times)	5	3
B Focal length (mm)	25	50
C Average Laser Power (W)	0.4	0.8
D Pulse Repetition Rate (kHz)	10	5
E Engraving Speed (mm/min)	3000	5000

3.3 Experimental Layout and Data

The experimental layout is shown in Table 3. Each experimental trial was conducted with two replications. Since a narrower linewidth is preferred, the lower-the-better (LB) formulation is chosen. The equation for calculating S/N ratios for an LB characteristic (in decibels) is

$$S / N_{LB} = -10 \log(\frac{1}{r} \sum_{i=1}^{r} y_i^2) \quad (1)$$

where r is the number of tests in a trial, and y_i is the value for the ith test in that trial. High signal-to-noise ratios are always preferred in a Taguchi experiment. For a Lower-the-Better characteristic, this translates into lower process average, improved consistency from one unit to the next, or both. The measured results of engraving linewidths and the S/N ratios obtained from equation (1) for each experimental trial are shown in Table 3.

Table 3 Experimental layout and raw data

Trial No.	Column No.					Linewidth (μm)		S/N (dB)
	1	2	4	8	15			
	Factor							
	A	B	C	D	E			
1	5	25	0.4	5	3000	32.0	32.0	-30.1
2	5	25	0.4	10	5000	25.0	23.0	-27.6
3	5	25	0.8	5	5000	32.0	30.0	-29.8
4	5	25	0.8	10	3000	68.5	68.0	-36.7
5	5	50	0.4	10	5000	20.5	22.0	-26.6
6	5	50	0.4	5	3000	23.5	22.5	-27.2
7	5	50	0.8	10	3000	21.0	23.0	-26.9

8	5	50	0.8	5	5000	23.0	19.5	-26.6
9	3	25	0.4	10	5000	27.5	25.5	-28.5
10	3	25	0.4	5	3000	33.5	37.0	-31.0
11	3	25	0.8	10	3000	34.5	36.5	-31.0
12	3	25	0.8	5	5000	36.5	34.0	-31.0
13	3	50	0.4	10	3000	44.0	48.0	-33.3
14	3	50	0.4	5	5000	40.0	44.5	-32.5
15	3	50	0.8	10	5000	51.5	53.0	-34.4
16	3	50	0.8	5	3000	67.5	67.5	-36.6

4 ANALYSIS AND DISCUSSION

4.1 Anova of S/N Ratios

The ANOVA of S/N ratios is shown in Table 4. The strategy of "pooling up" is used [8]. In the table, Df is the number of degrees of freedom, S is the sum of squares of source, V is the variance of source, F is the variance ratio, S' is the pure sum of squares of source, ρ is the percent contribution of source, and "epooled" is the pooled estimate of experimental error.

Table 4 ANOVA table

Source	Pool	Df	S	V	F	S'	r
A	[N]	1	44.46	44.46	17.10**	41.85	24.57
B	[Y]	1	0.17	0.17			
C	[N]	1	16.27	16.27	6.26*	13.67	8.02
D	[Y]	1	4.70	4.70			
E	[N]	1	15.62	15.62	6.01*	13.02	7.64
A×B	[N]	1	65.47	65.47	25.19**	62.87	36.89
EPOOLED		11	28.58	2.60		38.99	22.88
TOTAL		15	170.40				100.00

*At least 95% confidence, **At least 99% confidence

4.2 Significance of Each Source

The purpose of the analysis is to determine those factors/interactions that have strong effects on the engraving linewidth. Because the effect of a factor/interaction is equal to the difference between the average S/N ratios for each level, it can be observed from Fig. 1 that Factor A (beam expansion ratio) and the interaction between Factor A (beam expansion ratio) and Factor B (focal length) present the strongest effects. Statistically, only four effects are significant and they are ranked in the following order: A×B, A, C, E.

Figure 1 Response graphs for major effects and major interactions

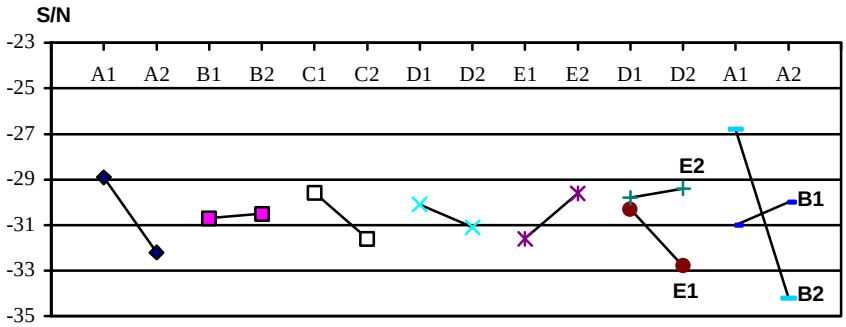

Before determining the recommended levels for Factor A and Factor B, the interaction effect between the Factors A and B has to be analysed. Since Factor B is a weak factor by itself, its preferred level will be based purely on the interaction A×B. From the interaction graph shown in Fig. 1, the intersecting lines for A×B indicate that there is indeed a strong interaction effect between factors A and B. Clearly, A1B2 is the preferred combination as high S/N ratios are required. Similarly, C1 and E2 are the preferred settings.

If only the effect of Factor D is considered, D1 and D2 make no significant difference as shown in Fig. 1, i.e., D can be set at either level. Physically, at a lower pulse repetition rate of 5 kHz (Level D2), the peak power is higher and the pulse width is shorter than that obtained at a higher frequency of 10 kHz (Level D1). The heat affected zone has been found to be smaller, and the corresponding engraving quality is better. Therefore, D2 has been selected to be the preferred setting. A more detailed discussion of the effect of pulse repetition rate (PRR) is given in section 4.3.3.

Thus, the recommended factor levels are A1, B2, C1, D2, and E2.

If we define the predicted signal-to-noise ratio based on the selected levels of the strong effects as η, the prediction equation can be written as [8]:

$$h = \overline{A_1 B_2} + \overline{C_1} + \overline{E_2} - 2\overline{T} \qquad (2)$$

Confidence interval around the estimated mean is [8]

$$CI = \sqrt{F_{a;1,v_e} Ve \left(\frac{1}{n_{eff}} + \frac{1}{r} \right)} \qquad (3)$$

where r is the sample size for the confirmation experiment, α is the risk level, where confidence = 1 - α, Ve is error variance, and n_{eff} = 4. For our confirmation test, α = 95%, r = 3, $F_{\alpha;1,ve}$ = 4.84, and Ve = 2.60.

Substituting the values, we get η = -24.81 dB and CI = 2.71 dB. That is, assuming no variability, the predicted average linewidth is 17.4 μm and the 95% confidence interval for the expected yield is $\{12.74\ \mu m \langle \overline{X} \langle 23.77\ \mu m\}$.

In order to confirm the prediction, an experiment using the recommended settings was conducted three times. The readings obtained were 18.0 μm, 19.0 μm and 17.0 μm, respectively. The average linewidth was 18.0 μm and the corresponding S/N ratio was -25.11 dB.

4.3 Discussions

4.3.1 Factors Affecting Engraving Linewidth

The engraving linewidth is dependent on power density, interaction time, and the evaporation threshold of the material. For a given pulse energy, E, the peak power is calculated by

$$P = \frac{E}{t} \qquad (4)$$

where t is the interaction time. The radial intensity variation of a Gaussian beam with spot size 2ω is given by [12]

$$I(r) = I_0 e^{-2r^2/w^2} \tag{5}$$

where I_0 is the intensity at r=0. The total power in an optical beam can be obtained by integrating over the cross-sectional area, that is,

$$P = \int_0^{2p} dq \int_0^{\infty} rI(r)dr = 2\pi\omega^2 I_0 \tag{6}$$

However, the engraving linewidth does not depend on the beam waist alone. It is also dependent on the evaporation threshold, as illustrated in Fig. 2 for two theoretical settings. In the diagram, Beam 1 has a smaller beam waist than Beam 2, but Beam 1 is able to produce a larger spot size on the substrate than that produced by Beam 2.

Figure 2 Laser beam distributions

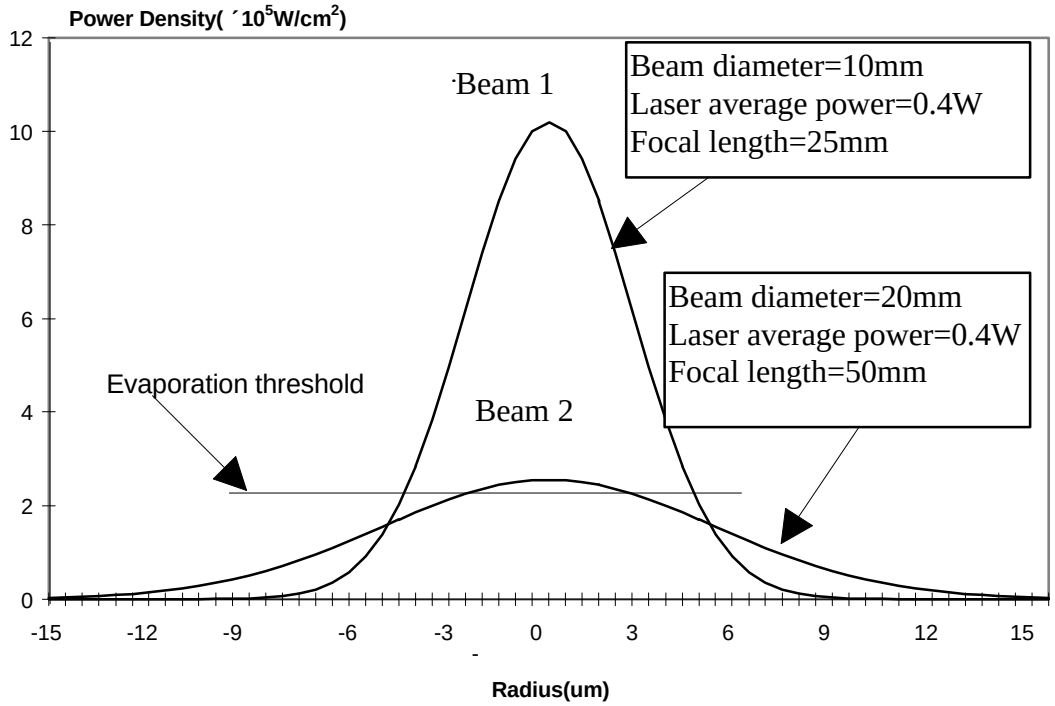

4.3.2 Effects of Beam Expansion Ratio and Focal Length

The reason that a significant interaction exists between the beam expansion ratio (Factor A) and focal length (Factor B) is that the two factors determine the focal spot size and the depth-of-focus. For a focused laser beam with a TEM_{00} mode, the theoretical spot size, s, is approximately given as [13]

$$s = \frac{2lf}{d} \tag{7}$$

where λ is the laser wavelength, d is the diameter of the beam entering the lens, and f is the focal length of the lens. On the other hand, d is directly proportional to the beam expansion ratio M, that is

$$d \propto M \tag{8}$$

Hence, we get

$$s \propto \frac{f}{M} \tag{9}$$

Therefore, the shorter the focal length and the bigger the beam expansion ratio, the smaller the focused spot size should be. But another Factor Affecting the focused spot size is spherical aberration. At the paraxial focus, the marginal ray has a diameter TSA (transverse spherical aberration) which may be calculated from [14]

$$TSA = 4K(n,q,p)\left(\frac{d}{f}\right)^3 S_2 \qquad (10)$$

where S_2 is the distance of the image to the lens, and the factor K(n,q,p) depends on the refractive index n of the lens, the shape factor q of the lens and the way in which the lens is used, which is indicated by the conjugate factor p. When the smallest diameter of the laser beam is sought, however, its diameter is only a quarter of the TSA which is obtained by defocusing to obtain the circle of least confusion. Therefore, for uncorrected but cheaper lenses, such as the ones used in our experiment, spherical aberration is more important than the diffraction effect in focusing the laser beam. Since the lens with focal length of 50 mm (Level B2) in our experiment gave similar results to those obtained by the lens with focal length of 25 mm (Level B1), this may indicate that the effects of spherical aberration, beam divergence, and diffraction effects may counteract with one another to give approximately the same focused spot size.

In order to test the effect of lens aberration for the 25 mm focal length lens, two comparative experiments were carried out. A linewidth of 26 μm was obtained at the parameters of beam expansion ratio of 5 ×, focal length of 25 mm, average power of 0.33 W, engraving speed of 3500 mm/min, and pulse repetition rate of 25 kHz. An aperture with a diameter of 6 mm was then placed in front of the focal lens, and a linewidth of 10.4 μm was obtained using the same parameters as above, which was very close to the theoretical spot size of 8.83 μm. Therefore, lens aberration is likely to have caused an enlarged focal spot size when compared to theoretical prediction. From the Taguchi experiment, it is observed that the preferred condition is A1B2 (beam expansion ratio of 5 × and focal length of 50 mm).

4.3.3 Effects of Average Laser Power, Pulse Repetition Rate and Engraving Speed

The main effects of average laser power (Factor C) and engraving speed (Factor E) are found to be statistically significant. Physically, for the NEC Q-switched Nd:YAG laser, the laser power and the pulse duration are controlled by changing the pulse repetition rate. The variation of average power, peak power, and pulse width with PRR are shown in Fig. 3. Typically, at a pulse repetition rate of 5 kHz, the pump current of 26 A across the flashlamp in the Nd:YAG laser system produces a pulse duration of 100 ns, laser average power of 5.1 W, and peak power of 10.2 kW. However, the values would change to 155 ns, 6.2 W and 4.0 kW at a pulse repetition rate of 10 kHz, as shown in Fig. 3. Note that, however, the actual laser power delivered to the specimen is further controlled by the use of a power attenuator. From the Taguchi experiment, a laser average power of 0.4 W at the workpiece is preferred.

Figure 3 Laser performance at different pulse repetition rate: (a) peak power and average power; (b) pulse width

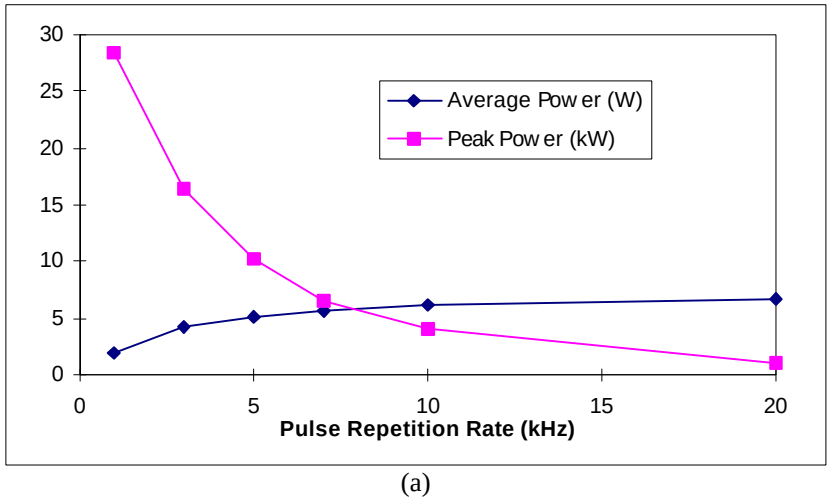

(a)

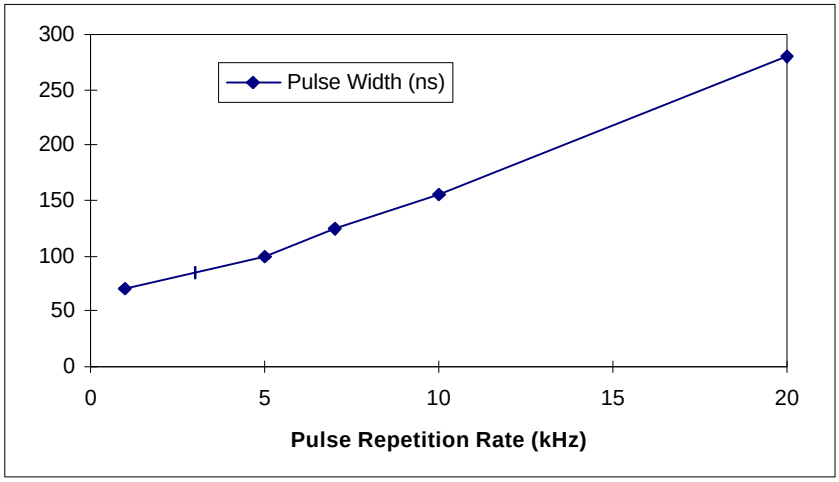

(b)

The PRR and the engraving speed together determine the percentage overlap in the laser spots. A good deal of overlap can ensure that the engraving lines are continuous and that spattering will be kept small. If the percentage overlap (in %) is defined as μ = x/s, then [15]

$$m = \frac{x}{s} = \left(1 - \frac{l}{s}\right) \times 100\% \tag{11}$$

where *s* is the spot size, *x* is overlap length, and *l* is the centre-to-centre spacing between the pulsed spots, which is given by

$$l = \frac{v}{PRR} \tag{12}$$

where PRR is the pulse repetition rate in pps, and v is the engraving speed in m/sec.

Therefore, the spot size is related to engraving speed and pulse repetition rate by

$$s = \left(\frac{100}{100 - \mu}\right)\frac{v}{PRR} \tag{13}$$

Geometrically speaking from Eq. (13), smaller line widths can be obtained by slow engraving speed and high pulse repetition rate. However, in the Taguchi experiment conducted, narrow linewidth was obtained for a higher engraving speed of 5000 mm/min (E2). The effect of PRR (Factor D) was found not to be statistically significant. These anomalies could result from the following considerations:

(a) Eq. (13) comes from geometrical derivation, i.e., it relates to the fact but does not explain the causes.

(b) At a faster speed of 5000 mm/min (E2), the interaction time between the laser beam and the coated substrate is smaller than that at a slower speed of E1. Thus, the heat-affected-zone is small resulting in a narrower linewidth.

(c) Some interaction effects may exist as evidenced by the D×E interaction graph shown in Fig. 1, and by the fact that the epooled experimental variation amounts to 22.88% of the total, as shown in Table 4.

5 CONCLUSION

Using the Taguchi method, the linewidth for laser micro-engraving of photomasks was optimized. An L16 orthogonal array was used to accommodate the experiments. The results revealed that the beam expansion ratio, the average laser power, the engraving speed, and the interaction between beam expansion ratio and focal length could significantly affect the engraving linewidth. By taking into consideration of physical effects, the optimal levels were chosen to be A1, B2, C1, D2, and E2, corresponding to beam expansion ratio of 5×, focal length of 50mm, laser average power of 0.4W, pulse repetition rate of 5kHz and engraving speed of 5000mm/min.

ACKNOWLEDGEMENT

The authors would like to thank Vikay Industrial Pte Ltd of Singapore for providing the photomask samples and the technical assistance rendered by the Advanced Machining Group of Gintic Institute of Manufacturing Technology .

REFERENCES

1 Glendinning, W. B. and Helbert, J. N. (1991) *Handbook of VLSI Microlithography: Principles, Technology and Applications*, Noyes Publications, New Jersey.
2 White, A. T. (1991) 'Evolution of the photomask industry', Proc. of SPIE, Vol. 1604, pp. 2 -23.
3 Growley, R. T. (1986) 'Laser fabrication of photomasks for hybrid circuits', Proc. of SPIE, Vol. 611, pp. 18-22.
4 Speidell, J. L., Cordes, S. A., and Ferry, A. (1994) 'An improved excimer laser pattern generator for photomask fabrication', Proc. of SPIE, Vol. 2322, pp. 66 -78.
5 Gauthier, R., Chroostowski, J., Paton, B., and Cada, M. (1986) 'Mask making using a laser writing system', Proc. of SPIE, Vol. 704, pp .91 -93.
6 Duley, W. W. (1983) *Laser Processing and Analysis of Materials*, Plenum Press, New York.
7 Chen, Y. H.,. Chen, W. L and Tam, S. C. (1995) 'Calculation of optical parameters in laser engraving of photomasks', International Conference on Optoelectronics and Lasers, Oct. 1995, Hangzhou, China, pp. 365-368.
8 Ross, R. J. (1989) *Taguchi Techniques for Quality Engineering*, McGraw-Hill, New York.
9 Ryan, N. E. (1988) *Taguchi Methods and QFD: Hows and Whys for Management*, ASI Press, Michigan.
10 Peace, G. S. (1992) *Taguchi Methods: a Hands-on Approach*, Addison-Wesley Publishing Company, Inc., Massachusetts.
11 Tam, S. C., Yeo, C. Y., Jana, S., Lau, W. S., Lim, E. N., Yang, L. J., and Noor, Y. M. (1993) 'Optimisation of laser deep -hole drilling of Inconel 718 using Taguchi method', J. of Material Processing Technology, Vol. 37, pp. 741-757.
12. Koechnev, W.(1992) Solid-State Laser Engineering, Springer-Verlag, Berlin
13. Siegman, A. E. (1986) *Lasers*, Oxford University Press, London.
14. Nonhof, C. J. (1988) Material Processing With Nd:YAG Lasers, Electrochemical Publications Limited.
15 Milonni, P. W. and Eberly, J. H. (1991) *Lasers*, John Wiley & Sons Inc., New York.